

# A conserved activation element in BMP signaling during *Drosophila* development

Alexander Weiss<sup>1</sup>, Enrica Charbonnier<sup>2,3</sup>, Elín Ellertsdóttir<sup>1</sup>, Aristotelis Tsirigos<sup>4</sup>, Christian Wolf<sup>5,6</sup>, Reinhard Schuh<sup>5</sup>, George Pyrowolakis<sup>2,3</sup> & Markus Affolter<sup>1</sup>

The transforming growth factor  $\beta$  (TGF- $\beta$ ) family member Decapentaplegic (Dpp) is a key regulator of patterning and growth in *Drosophila* development. Previous studies have identified a short DNA motif called the silencer element (SE), which recruits a trimeric Smad complex and the repressor Schnurri to downregulate target enhancers upon Dpp signaling. We have now isolated the minimal enhancer of the *dad* gene and discovered a short motif we termed the activating element (AE). The AE is similar to the SE and recruits the Smad proteins via a conserved mechanism. However, the AE and SE differ at important nucleotide positions. As a consequence, the AE does not recruit Schnurri but rather integrates repressive input by the default repressor Brinker and activating input by the Smad signal transducers Mothers against Dpp (Mad) and Medea via competitive DNA binding. The AE allows the identification of hitherto unknown direct Dpp targets and is functionally conserved in vertebrates.

Members of the transforming growth factor  $\beta$  (TGF- $\beta$ ) and bone morphogenetic protein (BMP) ligand family are important for a vast variety of biological processes<sup>1</sup>. These ligands signal through the structurally similar type I and type II serine-threonine kinase transmembrane receptors and the intracellular Smad proteins<sup>2,3</sup>. Upon phosphorylation, Smad transcription-factor complexes translocate into the nucleus and regulate the expression of target genes in cooperation with a plethora of cofactors<sup>4</sup>.

The best-characterized TGF- $\beta$ /BMP family member in *Drosophila* is Decapentaplegic (Dpp). One crucial molecular function of Dpp signaling is the repression of *brk*, a gene encoding the transcriptional repressor Brinker, which downregulates most Dpp target genes in the absence of signaling<sup>5–8</sup>. Repression of *brk* occurs at the transcriptional level via short so-called ‘silencer elements’ (SEs) in the *brk* gene; the *Drosophila* Smad proteins Mad and Medea bind as a trimer (two Mad, one Medea) to the SEs and recruit the corepressor Schnurri (Shn)<sup>9,10</sup>. Functional SEs also exist in the regulatory region of other genes that are efficiently repressed upon Dpp signaling, apparently independently of local cofactors<sup>9</sup>.

A number of Dpp-responsive enhancers have been analyzed at the molecular level. Most of these enhancers contain individual Smad-binding motifs and binding sites for locally restricted transcription factors<sup>11</sup>. Binding of trimeric Smad complexes has not been observed on any of these enhancers, and the simple nature of the single Smad-binding motif<sup>12–14</sup> does not allow for any reasonable genome-wide target gene prediction. This is in sharp contrast to the SE, which has been used successfully in *in silico* screens<sup>9</sup>.

Because we wanted to characterize the sequence requirements for widespread Dpp-induced activation, we dissected the regulatory

region of *dad*, which encodes the only *Drosophila* inhibitory Smad Daughters against Dpp and is induced by Dpp signaling in most embryonic and larval tissues<sup>15–17</sup>. Here we report on the identification of the regulatory regions of *dad* and the characterization of a short ‘activating element’, which is able to confer Dpp activity both in cultured cells and *in vivo* as well as conferring BMP responsiveness in zebrafish.

## RESULTS

### The *dad* gene is regulated by Dpp and Brk

In many cells in which the Dpp signaling pathway is inactive, Dpp target genes are repressed by direct binding of the Brk repressor protein to *cis*-regulatory elements. The mere removal of Brk in cells responding to high levels of Dpp signaling leads to the activation of certain target genes such as *omb* (optomotor blind) via ‘derepression’<sup>18</sup>. Other genes, such as *Ance* (better known as *Race*), are Brk-independently ‘directly activated’ by recruiting Smad complexes to *cis*-regulatory elements, where they cooperate with other activators<sup>19</sup>. It is likely that most Dpp-induced genes are regulated both by derepression and direct activation, as are *sal* (also called *spalt*)<sup>15,20</sup> and *zen*<sup>21</sup>, whose enhancers contain functional Smad-binding motifs as well as Brk-binding sites.

*dad* is a potential direct target of Brk. Expression of *dad* is induced in most embryonic and larval cells responding to Dpp and is complementary to the expression domains of *brk*<sup>8,15–17</sup> (Fig. 1a–d) and *dpp* (Supplementary Fig. 1b,c). To determine whether *dad* is directly activated by the Dpp pathway, we analyzed its expression in various genetic backgrounds (Supplementary Fig. 1d–l). From these experiments we concluded that *dad* integrates both Brk and Dpp input.

<sup>1</sup>Biozentrum der Universität Basel, Basel, Switzerland. <sup>2</sup>Institut für Biologie I and <sup>3</sup>Centre for Biological Signalling Studies (bloss), Albert-Ludwigs-Universität Freiburg, Freiburg, Germany. <sup>4</sup>Bioinformatics and Pattern Discovery Group, IBM T. J. Watson Research Center, Yorktown Heights, New York, USA. <sup>5</sup>Max-Planck-Institut für Biophysikalische Chemie, Göttingen, Germany. <sup>6</sup>Present address: Intervet Innovation GmbH, Drug Discovery, Schwabenheim, Germany. Correspondence should be addressed to G.P. (g.pyrowolakis@biologie.uni-freiburg.de) or M.A. (Markus.Affolter@unibas.ch).

Received 4 February; accepted 8 October; published online 13 December 2009; corrected online 27 December 2009 (details online); doi:10.1038/nsmb.1715

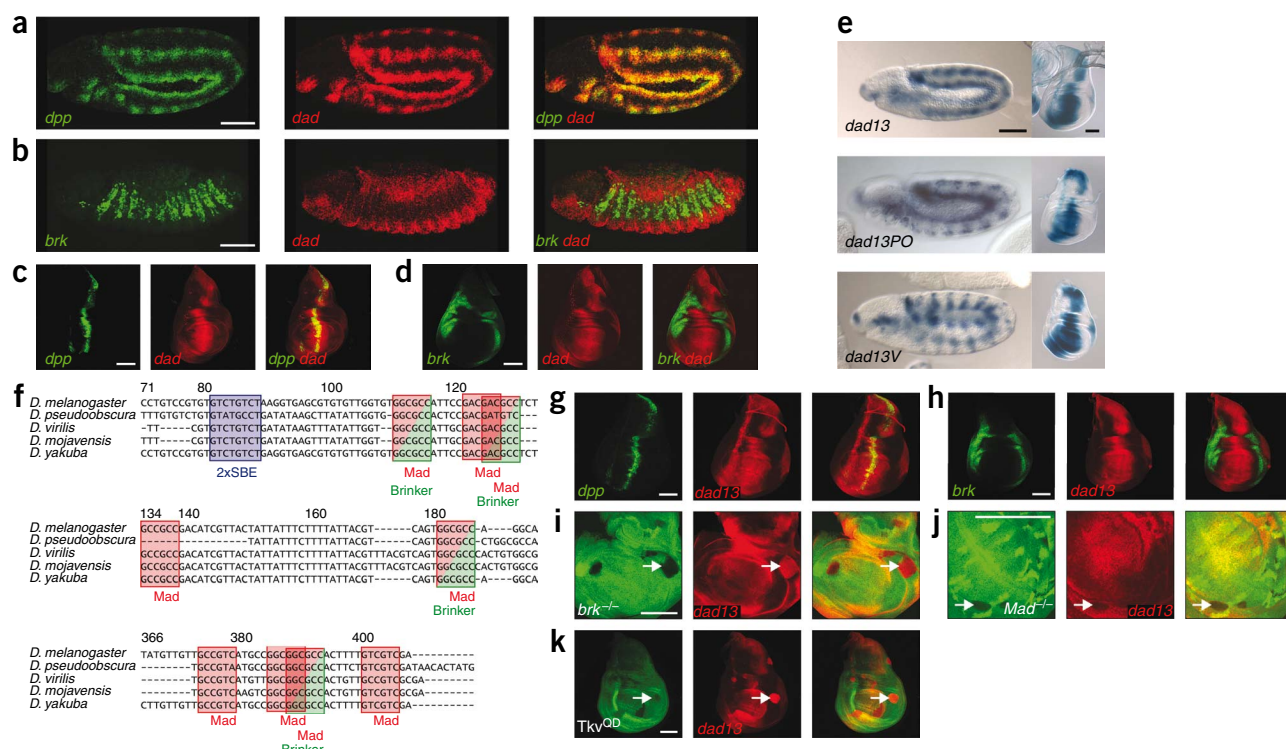


**Figure 1** Identification of the highly conserved minimal *dad* enhancer. (a–d) In the embryo, the expression patterns of *dad* and *dpp* overlap (as shown for stage 11 in a), whereas the expression domains of *dad* and *brk* are mutually exclusive (shown for stage 14 in b). The same holds true for the wing imaginal disc (c,d). Expression domains were visualized by *in situ* hybridization of endogenous transcripts and reporter antibody stainings. (e) The homologous genomic regions of the 520 bp minimal *dad* enhancer Dad13 were cloned from *D. pseudoobscura* (Dad13PO) and *D. virilis* (Dad13V) and transformed as *lacZ* reporter constructs into *D. melanogaster*. Expression patterns (detected by *in situ* hybridization and Xgal staining) were very similar to that of Dad13. (f) Sequence alignment of two conserved regions within Dad13, including a tandem Smad-binding element (SBE, blue) as well as putative Mad (red) and Brk binding sites (green). Numbers refer to the nucleotide position within Dad13. (g–k) Whereas the expression domain of the *dad13* reporter centered on the *dpp* expression domain (g), the expression patterns of *brk* and *dad13* were complementary (h). Clones mutant for *brk* ectopically upregulated *dad13* (i), whereas cells mutated for *Mad* did not express *dad13* (j). Clonal expression of the constitutively active Dpp receptor *Tkv<sup>QD</sup>* led to strong cell-autonomous induction of *dad13* (k). Mutant clones were indicated by loss of a GFP (i,j) or a CD2 (k) marker (arrows show examples). Scale bars, 75  $\mu$ m.

### Identification of the *dad* enhancer

In order to identify the regulatory regions of *dad*, we analyzed the expression of *lacZ* reporter constructs in transgenic flies. This resulted in the isolation of a 520-base-pair (bp) construct, Dad13, that drove *lacZ* expression in a pattern virtually identical to that of endogenous *dad* (Supplementary Fig. 2). Dad13 consists of two regions of about 150 bp each, which are highly conserved among distantly related *Drosophila* species and separated by a poorly conserved stretch of DNA (Supplementary Fig. 2a).

To determine whether the high degree of conservation was reflected in similar expression patterns, we cloned the corresponding genomic regions from *Drosophila pseudoobscura* (Dad13PO) and *Drosophila virilis* (Dad13V) (see Supplementary Table 1). The *lacZ* reporter plasmids containing these enhancers were then transformed into *Drosophila melanogaster*. The resulting expression patterns in the embryo and larval discs highly resembled those induced by Dad13 (Fig. 1e), suggesting an important function for the conserved elements.

Because genetic analyses indicated regulation of *dad* by both *brk* and *dpp*, we screened Dad13 for the experimentally derived Brk consensus sequence (T)GGCGYY (all sequences are given in 5'-to-3' orientation)<sup>18,22</sup>, the simple Smad-binding element (SBE) GTCT<sup>13,14</sup> and the sequence GRCGNC, which has been shown to recruit *Drosophila* Mad proteins<sup>9,10</sup>. Most of the sites we identified fall into the two highly conserved regions (Fig. 1f). Notably, all of the

three conserved potential Brk sites overlap with Mad sites, suggesting a possible competition for binding of the two proteins, as has been reported for other Dpp-responsive enhancers<sup>21,23,24</sup>.

To investigate whether the same regulatory mechanisms apply for Dad13 as for the *dad* gene itself, we analyzed its activity in mutant backgrounds and compared it to the expression patterns of *dpp* and *brk* (Fig. 1g–k). The expression pattern of the *dad13* reporter gene closely reflected *dad* expression in the wing imaginal disc. As expected for an enhancer repressed by Brk, the expression domains of *brk* and *dad13* were largely complementary. Furthermore, *dad13* was derepressed in clones mutated for *brk*. Cells that lacked the Mad protein did not express *dad13*, whereas clones expressing the constitutively active receptor *Tkv<sup>QD</sup>* strongly upregulated *dad13*. The same responses to ectopic activation of the Dpp pathway and expression of *brk* were observed in the embryo (data not shown).

### A Mad–Medea complex binds to the *dad* enhancer

To identify the sites at which Smad complexes and Brk regulate expression, we subdivided Dad13 into oligonucleotides of 40–70 bp in length and tested purified DNA-binding domains of Mad, Medea and Brk (Mad-MH1, Medea-MH1 and Brk-DBD, respectively) in electrophoretic mobility shift assays (Fig. 2a,b). All fragments containing putative Brk sites (S3, S4 and S7) were able to interact strongly with Brk-DBD. Mad-MH1 and Medea-MH1, however, were substantially recruited only to S2 (containing

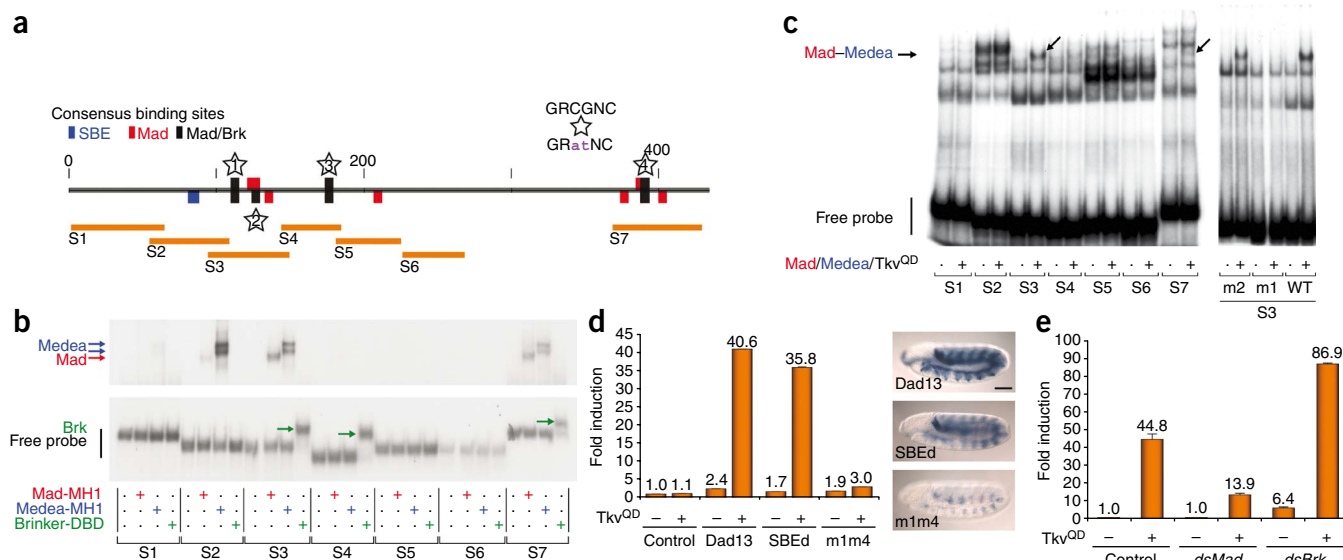


**Figure 2** Dad13 is directly regulated by Mad–Medea and Brk. (a) Overview of the generated Dad13 subconstructs S1–7. The placement of the color bars above or below the line indicates the orientation of the respective binding motif. Stars mark the Mad/Brk sites that were mutated from GRCGNC to GRATNC. The tandem SBE was converted from GTCTGTCT to GTATTCT. (b) Brk DNA-binding domain (Brk-DBD) was efficiently recruited to all three subfragments containing predicted Brk binding sites (green arrows), whereas Mad and Medea MH1 DNA binding domains bound only fragments S2, S3 and S7. (c) Binding of a full-length Mad–Medea complex was observed only for S3 and to a lesser extent for S7 (arrows). Mutation of Mad/Brk site 2 (m2) had no effect on binding, whereas mutation of site 1 (m1) completely abolished complex formation with Mad–Medea. (d) Upon cotransfection of a plasmid encoding Tk<sup>QD</sup>, Dad13 strongly drove expression of luciferase in S2 cells. Mutation of the SBEs had only little effect, in contrast to destruction of Mad/Brk sites 1 and 4. Similar results were observed in the embryo, where only destruction of the two Mad/Brk sites strongly reduced *lacZ* reporter expression (detected by antibody staining). Scale bar, 75  $\mu$ m. (e) RNAi-mediated downregulation of *Mad* in S2 cells transfected with Dad13 reporter plasmid reduced the effect of Tk<sup>QD</sup>, whereas downregulation of *brk* led to an increase in reporter gene expression. Control dsRNA had no effect. Luciferase reporter activity is plotted as the mean  $\pm$  s.d. of duplicates from a representative experiment.

a tandem SBE), S3 and S7, which both contained clusters of potential Mad sites. Mutational analyses of all positively tested DNA fragments revealed that Brk-DBD bound to the three predicted palindromic sites (1, 3 and 4), whereas Medea-MH1 mainly interacted with sites 1, 2 and 4 and Mad-MH1 mainly with sites 1 and 4 (Supplementary Fig. 3a,b).

To test whether the *dad* enhancer harbors high-affinity sites for full-length Smad complexes, we transfected tissue culture cells with plasmids encoding Mad, Medea and the constitutively active receptor Tk<sup>QD</sup> and used cell extracts derived from such cells for mobility shift experiments. We indeed found that S3 and to a lesser extent S7 were able to recruit a Mad–Medea complex (Fig. 2c, left). Destruction of the predicted Mad sites in S3 revealed that site 1 was responsible for Mad–Medea recruitment (Fig. 2c, right).

Because Dad13 drives expression of a reporter gene in S2 Schneider cells upon cotransfection of Tk<sup>QD</sup> (Fig. 2d), we were interested to see to what extent the identified sites contributed to activation of Dad13. Destruction of the tandem Smad-binding element (SBE<sup>d</sup>) had only a small effect on expression levels in transfected cells and transgenic embryos, consistent with the finding that full-length Smad complexes failed to bind S2 (Fig. 2c,d). However, mutation of Mad sites 1 and 4 was sufficient to nearly abolish expression in transfected cells as well as in the embryo (Fig. 2d). Expression in the wing imaginal disc was not completely abrogated but was reduced (data not shown). In accordance with the above findings, application of RNA interference against *Mad* reduced expression levels of *dad13* upon transfection with Tk<sup>QD</sup>, whereas targeting of *brk* increased both basal and Tk<sup>QD</sup>-induced transcription levels (Fig. 2e).

### Brk and Mad–Medea compete for binding

Due to the overlap of Brk and Mad–Medea sites in the *dad* enhancer, we speculated that these transcription factors compete for binding.

To test this, we performed competitive DNA-binding assays using S3, invariant amounts of Mad–Medea and increasing amounts of Brk. As expected, Brk was able to compete with Mad and Medea for DNA binding, and no complexes indicative of simultaneous Brk and Smad binding were seen (Fig. 3a).

Because all Brk sites in Dad13 are also putative Mad sites, and because Mad and Brk bind to very similar, but not identical, consensus sequences, we tested whether it was possible to convert a Mad/Brk site into an exclusive Mad site. We mutated the predicted Mad/Brk sites 1 and 2 (see Fig. 2a) to the sequence GACGTC, which still conformed to the Mad consensus sequence GRCGNC but no longer conformed to the Brk consensus sequence (T)GGCGYY. When short double-stranded oligonucleotides containing this sequence were subjected to shift assays, Brk binding was no longer detected, whereas Mad and Medea were still capable of binding (Fig. 3b and data not shown).

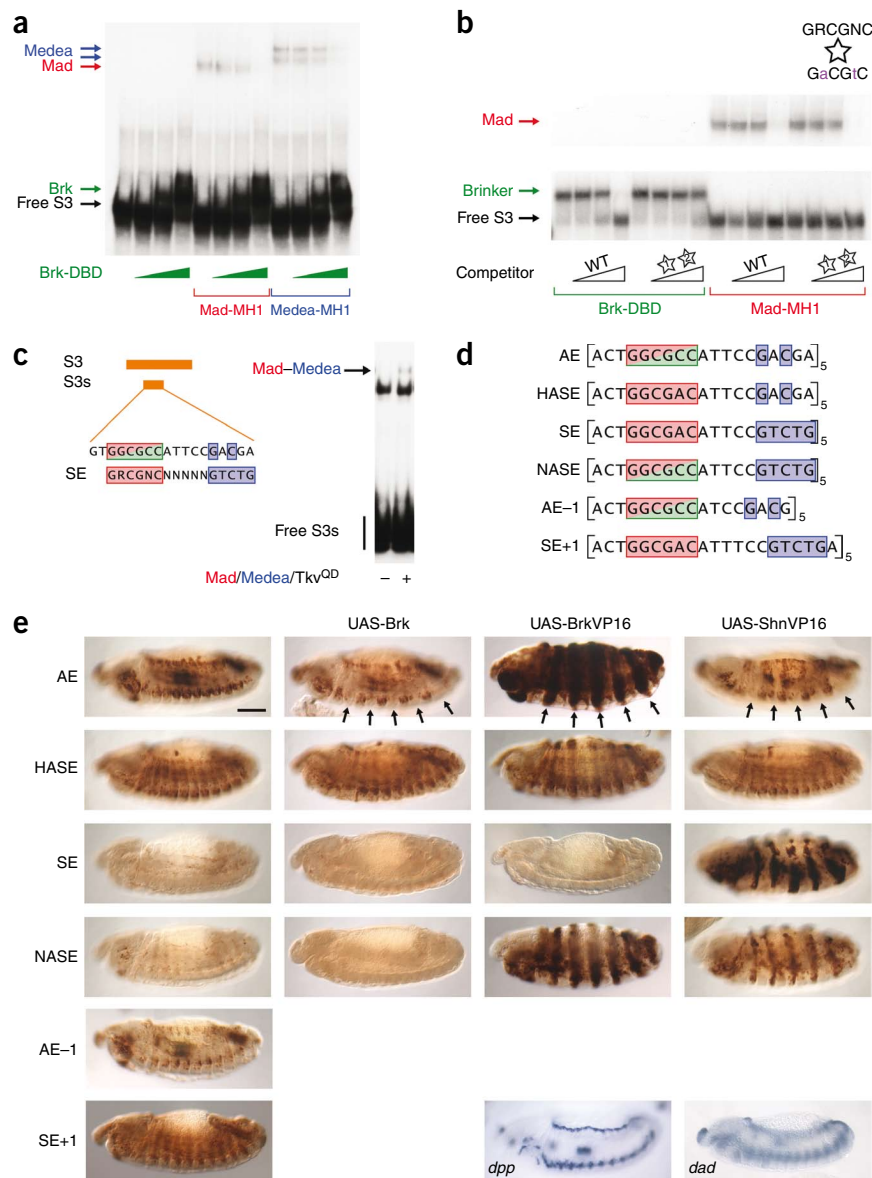
### A small activating element integrates Dpp and Brk input

To define more clearly the sequence element(s) responsible for Smad recruitment, we successively cropped S3. This ultimately led to the identification of the minimal fragment S3s (Fig. 3c). Unexpectedly, comparing the sequence of S3s to the silencer element (SE) revealed a noticeable similarity despite their completely opposing regulatory functions (activation versus repression). The ‘red box’ and ‘blue box’ of the SE, which recruit two Mad proteins and one Medea protein, respectively<sup>10</sup>, find their counterparts in the S3s construct. All three GNC motifs shown to be important for Smad binding turned out to be conserved between S3s and the SE, as well as the length of the linker between the red and blue box. However, there were two major differences. First, S3s lacks the second thymidine in the blue box, a residue crucial for the recruitment of the corepressor Shn in the SE<sup>9</sup>. Second, S3s harbors a Brk site, which



**Figure 3** A small DNA element integrates activating Smad and repressive Brk input.

(a) Recruitment of both Mad-MH1 and Medea-MH1 to S3 was clearly reduced in the presence of increasing amounts of Brk-DBD, indicating competitive binding. (b) Mutation of Mad/Brk sites 1 and 2 from GRCGNC to GACGTC strongly reduced the ability of the oligonucleotide to compete with wild-type S3 for Brk-DBD, but did not affect Mad-MH1 binding. (c) Subfragment S3s, including only Mad/Brk site 1 and a partial Mad site, was still able to recruit Smad proteins. Sequence comparison revealed a high similarity to the silencer element (SE). (d) Different reporter constructs based on AE and SE. Mad sites are depicted in red, Brk sites in green and Medea sites in blue. (e) Expression patterns induced by the pentamerized construct shown in **d** in transgenic stage 14 embryos, detected with a  $\beta$ -galactosidase antibody. At this developmental stage, the AE drove expression of the reporter gene in a manner highly similar to the endogenous *dad* expression. HASE activity lacked some of these features, but showed a marked expansion of ectodermal expression. Whereas SE and NASE did not induce *lacZ* expression, AE-1 did so to an extent similar to the AE. SE+1 activity resembled that of the HASE. Striped expression of Brk and the recombinant activators BrkVP16 and ShnVP16 had different predictable effects, dependent on the design of the construct. Expression patterns of *dad* and *dpp* (visualized by *in situ* hybridization) are shown for comparison. Scale bar, 75  $\mu$ m.



is not the case for any functional SE identified so far. On the basis of its function and its high similarity to the SE, we decided to name the motif in S3s the activating element (AE).

To investigate whether the AE alone was sufficient to confer Dpp signaling *in vivo*, we generated a pentamerized version of the AE (5xAE) and placed it in front of a *lacZ* reporter (Fig. 3d). In transgenic flies, this construct was indeed able to recapitulate the *dad* expression pattern in the late embryo in an unexpectedly accurate manner, including expression in two ectodermal stripes, in the gut and in anterior head structures (Fig. 3e).

### AE and SE are modular and convertible

The proposed modular nature of the AE and SE suggested that minimal changes in the sequences of either AE or SE would result in a different, predictable readout of Dpp activity. To test this, we created a number of additional pentamerized constructs that differed in several key aspects from the AE (Fig. 3d). The 'hyperactivated activating/silencer element' (HASE) harbors a single mutation that changes the Mad/Brk site to an exclusive Mad site. This construct was supposed to confer only activating Dpp responses and no repression via Brk. The 'nullified activating/silencer element' (NASE) includes both the nucleotides important for Shn binding as well as a perfect Brk site, and thus contains two potential sites for repressive input. Because it had been demonstrated that the SE linker length does not influence the formation of the Mad-Medea complex *in vitro*<sup>9</sup>, we also generated a construct with a linker of only 4 nucleotides (nt), AE-1. The repressive function of the SE depends on the

recruitment of Shn, which is only possible if the linker length is exactly 5 nt<sup>9</sup>. To investigate whether the SE, due to its similarity with the AE, also has an intrinsic potential for activation, we tested the construct SE+1, in which the linker length was increased to 6 nt. The capacity of all of these pentamerized constructs to drive a reporter gene in transgenic animals was compared to that of a similarly pentamerized version of the SE (Fig. 3e). The SE used in this experiment does not contain a Brk binding consensus sequence and should thus not be able to recruit Brk.

5xHASE, which is nearly identical to 5xAE but lacks the Brk site, was activated more weakly, but more widely, than 5xAE. 5xSE did not induce any expression at all and neither did 5xNASE, the construct identical to the SE but including a Brk site. The expression pattern induced by 5xAE-1 very much resembled that of 5xAE, with somewhat weaker expression in the two ectodermal stripes; this indicated that there is a certain linker-length flexibility for the AE, unlike for the SE, whose activity depends strictly on a linker length of 5 nt. In accordance with this, 5xSE+1 behaved totally different from 5xSE and acted in the embryo similarly to 5xHASE.

Based on the outcomes of our experiments described so far, we concluded that the AE is a Dpp-dependent activating element, which also confers repressive input via Brk. In contrast, the SE is a purely

repressive element, merely regulated by the Dpp pathway and Shn. To confirm this more firmly *in vivo*, we tested the behavior of the pentamerized constructs upon ectopic expression of different effector proteins (Fig. 3e). Indeed, striped expression of Brk (using a paired-Gal4 driver) led to local repression of 5xAE, but not of 5xHASE. Because both 5xSE and 5xNASE lacked reporter expression in transgenic flies, no effect could be seen upon ectopic expression of Brk. To see whether Brk interacts with these elements *in vivo*, we made use of a BrkVP16 fusion protein, in which the repression domain of the Brk protein was replaced with the activation domain of the herpes simplex virus protein VP16. Striped expression of BrkVP16 confirmed the results obtained for ectopic expression of Brk: although strong activation of 5xAE was observed, only weak activation of 5xHASE was seen. Furthermore, no effect was visible for 5xSE. 5xNASE, however, was indeed able to bind BrkVP16 *in vivo*, which resulted in strong activation of the 5xNASE construct in those cells in which the artificial activator was expressed.

Finally, we also generated and tested ShnVP16, a fusion protein consisting of the VP16 activation domain and a subfragment of the C-terminal

Shn domain (Shn<sup>CT</sup>), which is responsible for complex formation with the Smads on SEs. As expected, only 5xSE and 5xNASE showed ectopic activation in the presence of ShnVP16 (Fig. 3e), because only these two DNA sequence elements meet the sequence requirements for Mad–Medea–Shn complex formation. No effect was seen for 5xHASE, in contrast to 5xAE, which showed local repression where ShnVP16 was expressed. This observation can be explained by the upregulation of *brk* via its own endogenous SEs and again confirms the binding of Brk to the AE. Taken together, our results show that regulatory input can be separated both in the SE and in the newly identified AE. Two novel sequences, HASE and NASE, read out still different combinations of Dpp signaling input. Further characterization of HASEs and NASEs in the context of potential endogenous enhancers regulated by Dpp will provide more information on their role *in vivo*.

### Genome-wide search for conserved AEs

In view of the similarities between AE and SE, we wondered whether the AE would allow for the identification of previously unknown Dpp target genes as does the SE. Before performing this search, however, we sought to better define the AE consensus sequence by mutational analysis

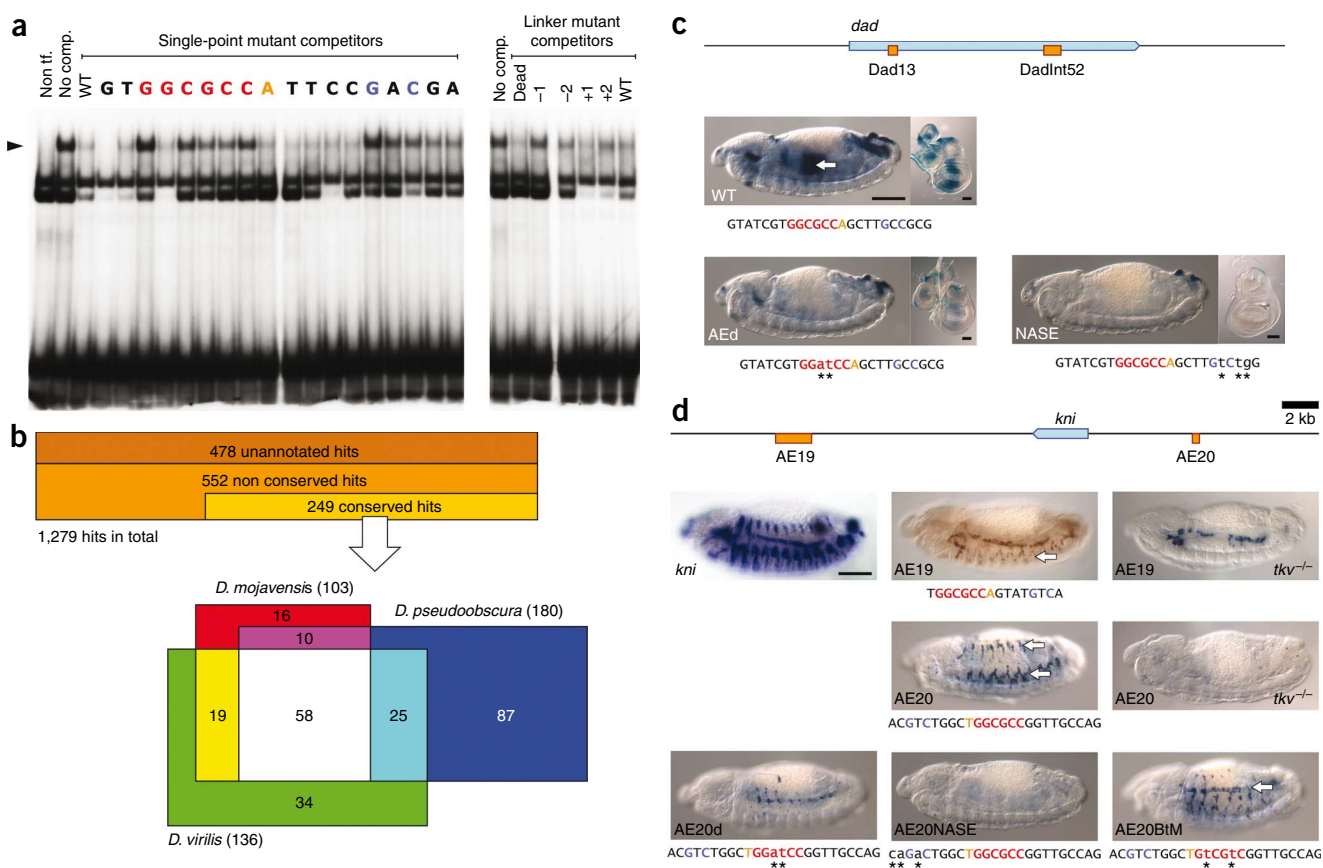


**Figure 4** Functional AEs are present in other enhancers. (a) Unlabeled single-point AE mutants were tested for their ability to compete for Mad–Medea complex formation with labeled AE (arrowhead). The lane under each nucleotide corresponds to the respective mutation. The first three lanes show control reactions with extract from nontransfected HEK 293 cells, without competitor and AE as competitor. Most of the nucleotides in the red and blue box interfered with complex formation, whereas exchanges of single or all nucleotides (“dead”) within the linker ATTCC did not. Linker-length variation affected complex assembly differently. (b) Results obtained from screening the genome of *D. melanogaster* for the AE sequence GGC GCCANNNGNCV and other species for conserved hits. (c) The activity of another *dad* enhancer, DadInt52, partially overlapped with that of Dad13. Mutation of 2 nt (AEd) strongly reduced activity in embryo (arrow) and imaginal discs, whereas transformation of the AE into a repressive NASE completely abolished Dpp-dependent reporter-gene expression. (d) AE19 and AE20 expression reflected aspects of the endogenous tracheal *kni* expression. In *tkv* mutant embryos, AE19 and AE20 reporter expression in ventral and dorsal structures (arrows) was lacking, whereas expression of AE19 in the visceral branch was only partially affected. Destruction of the AE in AE20 (AE20d) decreased reporter activity, whereas transformation of the AE into a NASE (AE20NASE) totally abrogated it. Changing the Brk/Mad site into an exclusive Mad site (AE20BtM) resulted in expansion of the tracheal expression into transverse connective and dorsal trunk (arrow). Scale bars, 75  $\mu$ m.

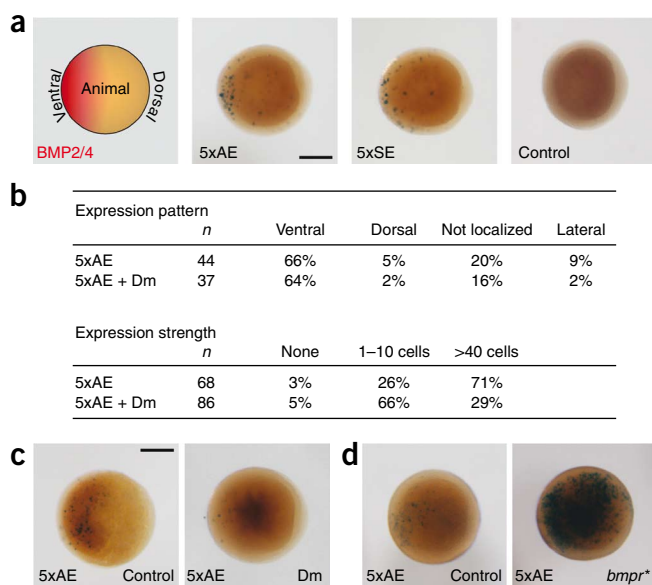


**Figure 5** The function of the AE is evolutionary conserved. (a) The schematic drawing of a 60% epiboly zebrafish embryo shows the ventrally localized distribution of BMP2 and BMP4. Both 5xAE and 5xSE were able to induce reporter-gene expression in the domain of BMP2 and BMP4 activity at comparable levels, unlike the reporter plasmid without enhancer. All embryos are photographed from the animal pole, ventral side to the left. (b,c) Application of the BMP inhibitor Dorsomorphin (Dm) to the medium did not alter the *lacZ* expression pattern induced by the AE, but strongly decreased the number of cells in which the AE was active. Two representative images are shown. (d) Coinjection of mRNA encoding the constitutively active BMP receptor IA led to dramatic expansion and upregulation of AE-induced reporter-gene expression. Scale bars, 200  $\mu$ m.

(Fig. 4a). The results confirmed once more the importance of the red and blue box as well as the flexibility of linker length and sequence. As the AE derived from the *dad* enhancer is able to recruit Brk, we also determined the best Brk site (Supplementary Fig. 3c,d) and integrated the resulting sequence of this site into the AE consensus. The outcome of these analyses was the consensus sequence GGCGCCANNNGNCV (V meaning any nucleotide except T), which also incorporated the fact that Shn should not be able to bind the AE.

For an *in silico* search using this consensus sequence, we used whole-genome alignments of *D. melanogaster* with *D. pseudoobscura*, *D. virilis* and *Drosophila mojavensis* from the UCSC Genome Browser (<http://genome.ucsc.edu>). Of a total of 1,279 AE hits in the *D. melanogaster* genome, 801 were found in annotated regions. Of these, 249 were conserved in at least one of the three distantly related *Drosophila* species and 58 in all of them (Fig. 4b and Supplementary Fig. 4). To validate a functional role of the conserved AE elements (see Supplementary Table 2 for an exhaustive list), we undertook a large-scale analysis.

### Identification of additional AEs in the *dad* and *kni* loci

To our surprise, our search revealed an additional putative AE in the *dad* locus, at the beginning of the fifth intron (Fig. 4c). To test whether this AE is indeed functional, a 1-kb enhancer construct (DadInt52) was used to drive a *lacZ* reporter gene. Activity of DadInt52 in the wing and haltere imaginal discs resembled the activity of Dad13, with repression at the dorsal-ventral compartment boundary (Fig. 4c). In the embryo, DadInt52 induced reporter expression in the head region as well as in endodermal cells, similarly to lab550, a well-characterized Dpp-regulated enhancer upstream of the *lab* (labial) gene<sup>25,26</sup>. To analyze the direct dependence of DadInt52 on Smad and Brk input, two different mutations were introduced. In one construct, the core nucleotides of the Mad/Brk site were altered (AEd). In the second construct (NASE), the thymidine nucleotide shown to be important for Shn recruitment was introduced, aiming to transform the AE embedded in DadInt52 into a purely repressive element. Expression in all imaginal discs decreased greatly upon mutation of the AE and was totally abolished when the AE was turned into an SE (Fig. 4c). In the embryo, expression was nearly abrogated for the construct with the destroyed AE and entirely suppressed for the one with a NASE, except for the four spots at the posterior end that remained unaffected for both constructs.

In summary, the AE identified within this second enhancer of the *dad* gene is crucial for the enhancer's function, and mutation of as few as 2 or 3 out of 1,000 nt is sufficient to abolish enhancer activity, providing a first validation of the hypothesis that Dpp target enhancers can be identified by genome-wide searches for AE elements.

Another gene that came up in our search was *kni*, which encodes the zinc-finger transcription factor Knirps<sup>27</sup>. Besides its well-studied role in patterning the early embryo, *kni* also functions in the formation of the tracheal system later in embryogenesis, where its expression is induced by Dpp signaling<sup>28</sup>. Two perfectly conserved AEs were found in the *kni* locus: in the 285-bp enhancer AE20 upstream of *kni* in proximity to the stripe enhancer<sup>29</sup> and in a 2-kb enhancer AE19 between the *kni* and *knrl* genes, 18 kilobases (kb) downstream of *kni* (Fig. 4d). Both enhancer constructs induced trachea-specific reporter-gene expression that mimicked aspects of endogenous *kni* tracheal expression. Whereas AE19 was active in the ventral tracheal placodes and the resulting tracheal branches as well as in visceral branches, AE20 was active in both dorsal and ventral tracheal placodes and branches. Consistent with Dpp-dependent regulation, ventral and dorsal expression of these reporter constructs was absent in *tkv* mutant embryos. To verify the importance of the AE, we focused on AE20 and introduced mutations similar to those described in the context of DadInt52, either destroying the AE (AE20d) or turning it into a NASE (AE20NASE). To investigate the role of Brk in the regulation of enhancer activity, we created a third mutation designed to convert the putative Brk/Mad site into an exclusive Mad site (AE20BtM). Expression of the reporter gene was strongly reduced upon destruction of the AE and completely gone when the AE was converted into a NASE (Fig. 4d). Notably, removing the Brk input without destroying the Mad site resulted in a dramatic expansion of the expression pattern; reporter expression was not only detected in the dorsal and ventral branches (though at slightly lower levels), but also in the tracheal cells in between (arrow in Fig. 4d, AE20BtM), namely those of the dorsal trunk, where Brk is active (data not shown). Altogether, our results suggest that the AE of this *kni* enhancer is an important site for direct activating Dpp signaling input. Further analysis revealed a potential cooperative effect with the selector proteins Trh and dARNT (Supplementary Fig. 5), which could represent a general theme for how AE-regulated enhancers induce tissue-specific expression.

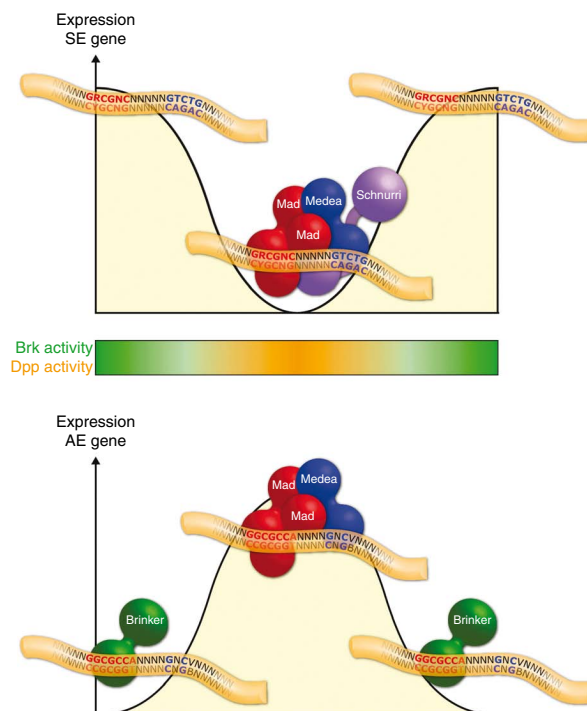
We have tested additional regulatory sequences with conserved AE elements in the loci of the *cv-2* (crossveinless-2), *elb* (elbow B), *pnr* (pannier) and *Doc* (Dorsocross) genes and found that many of them drove expression in cells in which the Dpp signaling pathway is active (Supplementary Figs. 6, 7).

### The function of the AE is phylogenetically conserved

SE-like BMP response elements inducing activation rather than repression have been found in the context of BMP-regulated vertebrate



**Figure 6** Despite their high similarity, SE and AE exert opposite functions. Genes controlled by an SE (top) are repressed in domains of high Dpp activity (center) via the assembly of a Mad–Medea–Shn complex. Outside the central Dpp domain, low amounts of activated Smad proteins fail to bind to the SE, and repression is relieved. The best-studied example of an SE-regulated gene is *brk*. Minimal differences in the sequence of the AE (with regard to the SE) still allow for binding of a Mad–Medea complex but prohibit the recruitment of the corepressor Shn. As a result, genes such as *dad* that are regulated by an AE (bottom) are activated in domains of high Dpp activity. Furthermore, Brk (whose expression is repressed by Dpp signaling) is able to bind to the AE in regions of low Dpp activity, thereby competing with Smad proteins for binding and repressing AE-mediated expression. AE and SE represent a striking example of how subtle nucleotide variations can result in a drastic switch in transcriptional regulation.



genes, including *bambi*, *smad7* and the *Id* genes<sup>30</sup> or the *Xenopus Vent2* promoter<sup>31</sup>, where a role of Shn as an activator has been implied<sup>32</sup>. Given these findings, we decided to test whether the simple pentamerized AE also induced expression of a *lacZ* reporter gene in a BMP-dependent manner in a vertebrate model organism, and we used the zebrafish embryo for this purpose. We injected reporter plasmids into 1- to 2-cell zebrafish embryos and determined *lacZ* activity by bromochloro-indolyl-galactopyranoside (Xgal) staining at ~60% epiboly. 5xAE as well as 5xSE induced ventral expression of the reporter gene (Fig. 5a), suggesting a role for BMP in this activation. To verify this, we applied dorsomorphin, a drug shown to specifically counteract BMP-mediated phosphorylation of Smad1, Smad5 and Smad8<sup>33</sup>. Indeed, we registered a strong decrease in activity, while the expression domain remained unchanged (Fig. 5b,c). In contrast, coinjection of mRNA encoding the constitutively active BMP receptor IA led to ubiquitous activation of the reporter (Fig. 5d). These experiments clearly show that the AE we identified in different Dpp target genes in the fly functions as a BMP response element in the zebrafish embryo.

## DISCUSSION

### Identification of the AE as a Dpp response element

In our attempt to identify and functionally characterize a Dpp response element that is activated in many different tissues, we identified a 520-bp fragment within the second intron of the *dad* gene. This fragment induces an expression pattern very similar to that of the endogenous *dad* gene in embryonic, larval and adult tissues and contains evolutionarily conserved and largely overlapping binding sites for Smad and Brk proteins within a short sequence element we called activating element (AE). The Smad and Brk proteins bind in a competitive manner to the AE, a mechanism similarly proposed for *zen* and *Ubx* enhancer elements<sup>21,23,24</sup>. By precise targeted mutations, we were able to selectively abolish Brk binding and show that it is possible to unlink Smad and Brk input. Notably, the AE assembles a high-affinity trimeric complex of full-length Mad and Medea proteins. In *Drosophila*, such complexes have so far only been demonstrated for a so-called silencer element (SE)<sup>9</sup>. Therefore, we present here the first example of such complex formation on a short-sequence element in the context of a gene activated by Dpp.

The AE very closely resembles the SE, but despite their analogy, AE and SE differ in several key aspects. Because of the arrangement of the Smad binding sites, they are both able to recruit a complex of Mad and Medea. However, only the SE includes the second thymidine within the blue box, which is essential for the recruitment of the repressor Shn<sup>9</sup>. Furthermore, the AE identified in the *dad* enhancer is able to interact with the Brk repressor. Brk competes with Mad for binding to the red box of the AE, which fulfills the consensus sequence derived from analysis of the SE with regard to Mad binding

(GRCGNC) as well as the sequence for Brk binding (TGGCGYY). In contrast, Brk does not bind to the SEs described (ref. 9; this work). Thus, the AE and SE use a very similar sequence to exert opposite effects. Our results provide a striking molecular scenario for Dpp signaling readout, based on the assembly of a trimeric Smad complex and its recruitment of a corepressor (Shn) or its competition with a dedicated repressor of the pathway (Brk) (see Fig. 6).

### Aspects of the AE regulation

Because Smads have been reported to interact with other transcription factors to induce target-gene expression, and considering that transcriptional activation brought about by signaling is thought to depend on local coactivators<sup>34</sup>, it was not self-evident that a simple pentamerized AE would be sufficient to drive expression in such a specific pattern. This brings up the question of whether this activation is due to an intrinsic activation capability of the Smad proteins or to the recruitment of an unknown coactivator. So far we do not have any evidence that Shn, which has also been associated with activation in *Drosophila*<sup>16,35</sup>, acts on the AE. Owing to its sequence requirements, a biologically active C-terminal version, Shn<sup>CT</sup>, is not able to bind to the AE. Domains of human Shn with homology to the N-terminal regions of Shn (that are not included in Shn<sup>CT</sup>) were shown to bind to the SE<sup>31</sup>, which might indicate other, so far unknown, functions of *Drosophila* Shn. However, this is probably not the case in the context of the *dad* enhancer. This becomes evident when looking at *brk/shn* double mutants, where transcription of *dad* is activated and thus does not depend on Shn as a coactivator.

The AE consensus sequence GGCGCCA(N)<sub>4</sub>GNCV is based on the analysis and dissection of the element we identified in the *dad* enhancer. We demonstrated the usefulness of this consensus sequence for the identification of other enhancers directly activated by the Dpp pathway and showed that also variants of this sequence (such as HASE) allow for activation upon Dpp signaling. In addition, our data indicate that the function of the AE is not strictly dependent on linker length, which is in sharp contrast to the SE and in accordance with previous studies<sup>9,36</sup>. However, 5 nt might be the optimal spacing for Smad binding to the AE.

## The AE as an evolutionarily conserved *cis*-regulatory element

The AE shows how the binding sites of three distinct proteins (Mad, Medea and Brk) converged into a bipartite motif. Thus far, no Brk homolog has been identified in vertebrates. However, AE- and SE-like submotifs have been found in the enhancers of several vertebrate genes activated by BMP signaling, such as *smad7*, *bambi* or the *Id* genes<sup>30,37</sup>. The promoter region of the vertebrate *dad* homolog *smad7* is one of the best-analyzed BMP-regulated enhancers. After identification of the Smad-binding element (SBE)<sup>13,14</sup>, the existence of a palindromic tandem SBE GTCTAGAC, which confers BMP responsiveness by recruitment of Smad3 and Smad4, was reported for the human and mouse *smad7* enhancer<sup>38–41</sup>. Later, a sequence TGGCGCC within so-called BMP response elements of the vertebrate *smad7* enhancer was found to recruit Smad1<sup>30,42</sup>. Despite the large number of single Smad-binding motifs, no bipartite element has been reported, and the question of whether heteromeric Smad complexes are recruited to these sites has not been addressed. The fact, however, that the identified TGGCGCC sites appear in the context GGCGCCA(N)<sub>4</sub>GNC favors the existence of an element analogous to the AE within the vertebrate *smad7* gene.

## METHODS

Methods and any associated references are available in the online version of the paper at <http://www.nature.com/nsmb/>.

*Note: Supplementary information is available on the Nature Structural & Molecular Biology website.*

## ACKNOWLEDGMENTS

We are deeply thankful to B. Hartmann (University of Freiburg) for generously providing the flies transgenic for UAS-ShnVP16. Work in the lab of M.A. was supported by the Kantons Basel-Stadt and Basel-Land, by the Swiss National Science Foundation and by SystemsX.ch within the framework of the wingX RTD. Work in G.P.'s laboratory was supported by the German Research Foundation (SFB592) and the Excellence Initiative of the German Federal and State Governments (EXC294).

## AUTHOR CONTRIBUTIONS

A.W., E.C., E.E. and C.W. performed the experiments; A.T. and A.W. generated the bioinformatic data; A.W. and M.A. wrote the manuscript; M.A., G.P. and R.S. contributed to design and interpretation of the experiments and paid the bills.

Published online at <http://www.nature.com/nsmb/>.

Reprints and permissions information is available online at <http://npg.nature.com/reprintsandpermissions/>.

- Derynck, R. & Miyazono, K. *TGF- $\beta$  and the TGF- $\beta$  Family* (Cold Spring Harbor Laboratory Press, Cold Spring Harbor, New York, USA, 2007).
- Shi, Y. & Massague, J. Mechanisms of TGF- $\beta$  signaling from cell membrane to the nucleus. *Cell* **113**, 685–700 (2003).
- Schmierer, B. & Hill, C.S. TGF $\beta$ -SMAD signal transduction: molecular specificity and functional flexibility. *Nat. Rev. Genet.* **8**, 970–982 (2007).
- Feng, X.H. & Derynck, R. Specificity and versatility in tgf- $\beta$  signaling through Smads. *Annu. Rev. Cell Dev. Biol.* **21**, 659–693 (2005).
- Campbell, G. & Tomlinson, A. Transducing the Dpp morphogen gradient in the wing of *Drosophila*: regulation of Dpp targets by brinker. *Cell* **96**, 553–562 (1999).
- Jazwinska, A., Kirov, N., Wieschaus, E., Roth, S. & Rushlow, C. The *Drosophila* gene brinker reveals a novel mechanism of Dpp target gene regulation. *Cell* **96**, 563–573 (1999).
- Jazwinska, A., Rushlow, C. & Roth, S. The role of brinker in mediating the graded response to Dpp in early *Drosophila* embryos. *Development* **126**, 3323–3334 (1999).
- Minami, M., Kinoshita, N., Kamoshida, Y., Tanimoto, H. & Tabata, T. brinker is a target of Dpp in *Drosophila* that negatively regulates Dpp-dependent genes. *Nature* **398**, 242–246 (1999).
- Pyrowolakis, G., Hartmann, B., Muller, B., Basler, K. & Affolter, M. A simple molecular complex mediates widespread BMP-induced repression during *Drosophila* development. *Dev. Cell* **7**, 229–240 (2004).
- Gao, S., Steffen, J. & Laughon, A. Dpp-responsive silencers are bound by a trimeric Mad-Medea complex. *J. Biol. Chem.* **280**, 36158–36164 (2005).

- Pyrowolakis, G., Hartmann, B. & Affolter, M. TGF- $\beta$  family signaling in *Drosophila*. in *The TGF- $\beta$  Family* (eds. Derynck, R. & Miyazono, K.) 493–526 (Cold Spring Harbor Laboratory Press, Cold Spring Harbor, New York, USA, 2007).
- Kim, J., Johnson, K., Chen, H.J., Carroll, S. & Laughon, A. *Drosophila* Mad binds to DNA and directly mediates activation of vestigial by decapentaplegic. *Nature* **388**, 304–308 (1997).
- Shi, Y. *et al.* Crystal structure of a Smad MH1 domain bound to DNA: insights on DNA binding in TGF- $\beta$  signaling. *Cell* **94**, 585–594 (1998).
- Zawel, L. *et al.* Human Smad3 and Smad4 are sequence-specific transcription activators. *Mol. Cell* **1**, 611–617 (1998).
- Marty, T., Muller, B., Basler, K. & Affolter, M. Schnurri mediates Dpp-dependent repression of brinker transcription. *Nat. Cell Biol.* **2**, 745–749 (2000).
- Torres-Vazquez, J., Park, S., Warrior, R. & Arora, K. The transcription factor Schnurri plays a dual role in mediating Dpp signaling during embryogenesis. *Development* **128**, 1657–1670 (2001).
- Tsuneizumi, K. *et al.* Daughters against dpp modulates dpp organizing activity in *Drosophila* wing development. *Nature* **389**, 627–631 (1997).
- Sivasankaran, R., Vigano, M.A., Muller, B., Affolter, M. & Basler, K. Direct transcriptional control of the Dpp target omb by the DNA binding protein Brinker. *EMBO J.* **19**, 6162–6172 (2000).
- Xu, M., Kirov, N. & Rushlow, C. Peak levels of BMP in the *Drosophila* embryo control target genes by a feed-forward mechanism. *Development* **132**, 1637–1647 (2005).
- Barrio, R. & de Celis, J.F. Regulation of spalt expression in the *Drosophila* wing blade in response to the decapentaplegic signaling pathway. *Proc. Natl. Acad. Sci. USA* **101**, 6021–6026 (2004).
- Rushlow, C., Colosimo, P.F., Lin, M.C., Xu, M. & Kirov, N. Transcriptional regulation of the *Drosophila* gene zen by competing Smad and Brinker inputs. *Genes Dev.* **15**, 340–351 (2001).
- Zhang, H., Levine, M. & Ashe, H.L. Brinker is a sequence-specific transcriptional repressor in the *Drosophila* embryo. *Genes Dev.* **15**, 261–266 (2001).
- Kirkpatrick, H., Johnson, K. & Laughon, A. Repression of dpp targets by binding of brinker to mad sites. *J. Biol. Chem.* **276**, 18216–18222 (2001).
- Saller, E. & Bienz, M. Direct competition between Brinker and *Drosophila* Mad in Dpp target gene transcription. *EMBO Rep.* **2**, 298–305 (2001).
- Grieder, N.C., Marty, T., Ryoo, H.D., Mann, R.S. & Affolter, M. Synergistic activation of a *Drosophila* enhancer by HOM/EXD and DPP signaling. *EMBO J.* **16**, 7402–7410 (1997).
- Marty, T. *et al.* A HOX complex, a repressor element and a 50 bp sequence confer regional specificity to a DPP-responsive enhancer. *Development* **128**, 2833–2845 (2001).
- Rothe, M., Nauber, U. & Jackle, H. Three hormone receptor-like *Drosophila* genes encode an identical DNA-binding finger. *EMBO J.* **8**, 3087–3094 (1989).
- Chen, C.K. *et al.* The transcription factors KNIRPS and KNIRPS RELATED control cell migration and branch morphogenesis during *Drosophila* tracheal development. *Development* **125**, 4959–4968 (1998).
- Pankratz, M.J., Busch, M., Hoch, M., Seifert, E. & Jackle, H. Spatial control of the gap gene knirps in the *Drosophila* embryo by posterior morphogen system. *Science* **255**, 986–989 (1992).
- Karaulanov, E., Knochel, W. & Niehrs, C. Transcriptional regulation of BMP4 synexpression in transgenic *Xenopus*. *EMBO J.* **23**, 844–856 (2004).
- Yao, L.C. *et al.* Schnurri transcription factors from *Drosophila* and vertebrates can mediate Bmp signaling through a phylogenetically conserved mechanism. *Development* **133**, 4025–4034 (2006).
- Ross, S. & Hill, C.S. How the Smads regulate transcription. *Int. J. Biochem. Cell Biol.* **40**, 383–408 (2008).
- Yu, P.B. *et al.* Dorsomorphin inhibits BMP signals required for embryogenesis and iron metabolism. *Nat. Chem. Biol.* **4**, 33–41 (2008).
- Barolo, S. & Posakony, J.W. Three habits of highly effective signaling pathways: principles of transcriptional control by developmental cell signaling. *Genes Dev.* **16**, 1167–1181 (2002).
- Dai, H. *et al.* The zinc finger protein schnurri acts as a Smad partner in mediating the transcriptional response to decapentaplegic. *Dev. Biol.* **227**, 373–387 (2000).
- Gao, S. & Laughon, A. Flexible interaction of *Drosophila* Smad complexes with bipartite binding sites. *Biochim. Biophys. Acta* **1769**, 484–496 (2007).
- Korchynski, O. & ten Dijke, P. Identification and functional characterization of distinct critically important bone morphogenetic protein-specific response elements in the Id1 promoter. *J. Biol. Chem.* **277**, 4883–4891 (2002).
- Brodin, G., Ahgren, A., ten Dijke, P., Heldin, C.H. & Heuchel, R. Efficient TGF- $\beta$  induction of the Smad7 gene requires cooperation between AP-1, Sp1 and Smad proteins on the mouse Smad7 promoter. *J. Biol. Chem.* **275**, 29023–29030 (2000).
- Denisova, N.G., Pouppnot, C., Long, J., He, D. & Liu, F. Transforming growth factor  $\beta$ -inducible independent binding of SMAD to the Smad7 promoter. *Proc. Natl. Acad. Sci. USA* **97**, 6397–6402 (2000).
- Nagarajan, R.P., Zhang, J., Li, W. & Chen, Y. Regulation of Smad7 promoter by direct association with Smad3 and Smad4. *J. Biol. Chem.* **274**, 33412–33418 (1999).
- von Gersdorff, G. *et al.* Smad3 and Smad4 mediate transcriptional activation of the human Smad7 promoter by transforming growth factor  $\beta$ . *J. Biol. Chem.* **275**, 11320–11326 (2000).
- Benchabane, H. & Wrana, J.L. GATA- and Smad1-dependent enhancers in the Smad7 gene differentially interpret bone morphogenetic protein concentrations. *Mol. Cell. Biol.* **23**, 6646–6661 (2003).



## ONLINE METHODS

**Fly strains.** We used the mutant alleles *brk*<sup>M68</sup>, *shn*<sup>TD5</sup>, *tkv*<sup>str-II</sup>, *Mad*<sup>12</sup>, *trh*<sup>10512</sup>. For overexpression of UAS-TkvQD (ref. 43), UAS-Brk (ref. 6), UAS-BrkVP16 and UAS-ShnVP16 we used a prd-Gal4 driver line. For reporter analysis, we used *dad*<sup>P1883</sup> (ref. 17), *B14-GFP* (ref. 44), *X47* (ref. 5), *bam-GFP* (ref. 45) and *dpp-Gal4 UAS-CD8-GFP*.

**Clonal analysis.** We generated mutant clones by flipase-mediated mitotic recombination. Genotypes of dissected larvae were as follows. For *Mad* clones: *y w hsp70-flp; Mad*<sup>12</sup> *FRT40/ubi-nlsGFP FRT40; dad13-lacZ*. For *shn* clones: *y w hsp70-flp; FRT42D shn*<sup>TD5</sup> *FRT42D ubiGFP; dad13-lacZ*. For *brk* clones: *FRT18a brk/FRT18a ubiGFP; +; dad13-lacZ/MKRS, hsp70-flp*. We obtained Tkv<sup>QD</sup>-overexpressing clones in the wing disc with the flip-out technique using *hsp70-flp; +; dad13-lacZ/C765 UAS>CD2 y<sup>+</sup>>tkv*<sup>QD</sup> larvae.

**Immunohistochemistry and Xgal staining.** We incubated fixed *Drosophila* embryos with mouse antibody to GFP (anti-GFP; Roche) or anti-β-galactosidase (Promega or Cappel) using standard protocols. For alkaline phosphatase (AP) stainings, we used a secondary AP-conjugated mouse antibody (Abcam) and for horseradish peroxidase (HRP) stainings the Vectastain kit (Vector Laboratories). We performed Xgal color reactions with standard reagents. For fluorescent antibody stainings, we used rabbit anti-β-galactosidase (Cappel), 1:1,000; mouse anti-GFP (Roche), 1:1,000; mouse anti-CD2 (Caltag Laboratories), 1:500; goat anti-rabbit-Alexa 568 and goat anti-mouse-Alexa 499 (Invitrogen), 1:500; and DAPI (Sigma), 1:250. We mounted imaginal discs and ovaries in Vectashield mounting medium (Vector) and took images with a Zeiss LSM510 confocal microscope.

**In situ hybridization.** We carried out conventional *in situ* hybridization according to standard procedures, using digoxigenin-labeled RNA probes, an AP-conjugated digoxigenin antibody (Roche) and AP substrate. We performed double-fluorescence *in situ* hybridization and fluorescent *in situ* hybridization coupled to antibody staining as described<sup>46</sup>. We used a DIG POD antibody (Roche) and Tyramide Signal Amplification with HRP reagent (PerkinElmer).

**Computational analysis.** We performed an initial *in silico* screen using <http://www.flyenhancer.org><sup>47</sup>. To search for highly conserved AEs, we obtained sequence data and Gene Ontology annotations<sup>48</sup> from Ensembl release 52, based on genome assembly version BDGP 5.0 (March 2006). Whole-genome alignments of *D. melanogaster* (same assembly version) with *D. pseudoobscura* (Feb. 2006, Baylor CAF1), *D. virilis* (Feb. 2006, Agencourt CAF1) and *D. mojavensis* (Feb. 2006, Agencourt CAF1) were obtained from the University of California, Santa Cruz Genome Browser<sup>49</sup>.

For any motif, we located its instances in the *D. melanogaster* genome and checked its presence in the corresponding sequence in the respective aligning genome. A tolerance of 50 bp allowed for small stretches of misalignments. After removing instances inside annotated exons, we determined all proximate genes with the respective motif either 50 kb upstream or downstream of transcription start or within gene span if the gene was longer than 50 kb.

**Reporter transgenes.** We generated the initial Dad13, Dad13PO and Dad13V reporter transgenes by inserting the respective enhancer fragments between the XbaI and Asp718 sites of the plasmid px27 (ref. 50) and subsequent standard P-element transformation. All other reporter transgenes we generated using the phiC31-based integration system<sup>51</sup> with the landing platform ZH-86Fb (for AE20 also ZH-102D). We inserted enhancer and 5x constructs into an attBlacZ reporter vector, created by cloning a *lacZ* gene into the pUASTattB vector<sup>51</sup> and removing the upstream activator sequence (UAS) cassette. Genomic localization and respective primers for all constructs are shown in **Supplementary Table 1**.

**VP16 fusion proteins.** For BrkVP16, we inserted a fragment encoding the first 100 residues of Brk, a nuclear localization signal (NLS) and the VP16 activation domain into the expression vector pUAST<sup>52</sup> via its Asp718 and XbaI sites. We created ShnVP16 by fusing a NLS, the VP16 domain and the C-terminal 529 residues of Shn into the pUAST vector via its EcoRI and XbaI sites.

**Electrophoretic mobility shift assays.** We expressed recombinant Mad-MH1 and Medea-MH1 proteins (Mad residues 1–147 and Medea residues 16–355, fused to the GST moiety in the plasmid pGEX4T.1 (Pharmacia)) in *Escherichia coli* BL21 cells and purified them using glutathione-sepharose beads (Pharmacia). Brk-DBD comprises residues G43 to N101 and was purified as described<sup>53</sup>.

We used 0.8 μg Brk-DBD, 1 μg GST–Mad-MH1 or 0.4 μg GST–Medea-MH1. For the Brk/Smads competition assay, we applied 8 ng, 80 ng and 0.8 μg Brk-DBD. We obtained plasmids encoding GST-Trh and GST-dARNT from K. Saigo (Univ. of Tokyo)<sup>54</sup>. We performed electrophoretic mobility shift assays with recombinant proteins or *Drosophila* S2 cell extracts as described<sup>9</sup>. We cultured HEK 293 cells in DMEM + Glutamax (Gibco), supplemented with 10% (v/v) FBS (Gibco). We transfected 300,000 cells with 200 ng plasmid DNA (TkV<sup>QD</sup>, Mad and Medea in pcDNA3.1 (Invitrogen)) and treated them as described for S2 cells. The positions of the fragments S1–S7 with respect to Dad13 are (start–end): S1 (1–62), S2 (55–109), S3 (93–147), S4 (140–186), S5 (181–231), S6 (232–283) and S7 (370–433). To test the effect of the Brk/Mad to Mad site mutation, we used 0.24-, 2.4- and 24-fold excesses of unlabeled competitor. For definition of the AE consensus sequence, we provided a 200-fold excess of the respective unlabeled mutant competitors. We mutated bases from adenine to cytosine and guanine to thymine, and vice versa. Mutations of the ATTCC wild-type linker were CGGAA (dead), ATTC (–1), ATT (–2), ATTCCT (+1) and ATTCCTT (+2).

**Cell culture assays.** Insertion of the *hsp70* minimal promoter between the BglII and HindIII sites of the vector pGL3Basic (Promega) generated hsp70pGL3basic, in which we inserted Dad13 and mutant forms between XbaI and Acc65I sites. We maintained *Drosophila* S2 cells in Schneider's insect medium (Invitrogen) supplemented with 10% (v/v) FBS (Sigma) and transfected them using the Effectene Reagent (Qiagen). For reporter gene assays, we transfected 2 × 10<sup>6</sup> cells with 200 ng DNA (50 ng reporter plasmid, 5 ng *Renilla* luciferase plasmid, 5 ng expression plasmids, and the parental vector pAc5.1B/V5His up to 200 ng). For RNAi experiments, we treated cells with 50 ng TkV<sup>QD</sup> expression plasmid and dsRNA corresponding to nucleotides 658–1230 of the *Mad* and 983–1652 of the *brk* coding region as described<sup>9</sup>. We lysed cells 48 h after transfection and assayed lysates for firefly and *Renilla* luciferase activity using a Dual Luciferase Reporter Assay (Promega) and a TriStar LB491 luminometer (Berthold).

**Zebrafish Xgal staining.** We injected plasmids into one- and two-cell-stage embryos at a concentration of 10–40 ng μl<sup>–1</sup>. For ectopic activation, we coinjected 1–5 ng μl<sup>–1</sup> mRNA of BMPRIA (ref. 55). To inhibit BMP-mediated Smad phosphorylation, we applied 10 μM dorsomorphin (Sigma) to the medium when embryos reached the 1,000-cell stage. Embryos developed at 28.5 °C until ~60% epiboly before we fixed them in PBS, 2 mM MgCl<sub>2</sub> and 12% (v/v) glutaraldehyde for 8 min at 20–25 °C. For detection of β-galactosidase activity, we incubated embryos 3 h at 37 °C in 9 mM sodium phosphate (pH 7.2), 14 M NaCl, 0.9 mM MgCl<sub>2</sub>, 10 mM potassium ferrocyanide, 10 mM potassium ferricyanide, 0.05% (v/v) Triton X-100 and 80 mg ml<sup>–1</sup> Xgal.

43. Nellen, D., Burke, R., Struhl, G. & Basler, K. Direct and long-range action of a DPP morphogen gradient. *Cell* **85**, 357–368 (1996).
44. Müller, B., Hartmann, B., Pyrowolakis, G., Affolter, M. & Basler, K. Conversion of an extracellular Dpp/BMP morphogen gradient into an inverse transcriptional gradient. *Cell* **113**, 221–233 (2003).
45. Chen, D. & McKearin, D.M. A discrete transcriptional silencer in the bam gene determines asymmetric division of the *Drosophila* germline stem cell. *Development* **130**, 1159–1170 (2003).
46. Kosman, D. *et al.* Multiplex detection of RNA expression in *Drosophila* embryos. *Science* **305**, 846 (2004).
47. Markstein, M., Markstein, P., Markstein, V. & Levine, M.S. Genome-wide analysis of clustered Dorsal binding sites identifies putative target genes in the *Drosophila* embryo. *Proc. Natl. Acad. Sci. USA* **99**, 763–768 (2002).
48. Ashburner, M. *et al.* Gene ontology: tool for the unification of biology. The Gene Ontology Consortium. *Nat. Genet.* **25**, 25–29 (2000).
49. Kent, W.J. *et al.* The human genome browser at UCSC. *Genome Res.* **12**, 996–1006 (2002).
50. Segalat, L., Berger, G. & Lepesant, J.A. Dissection of the *Drosophila* pourquoi-pas? promoter: complex ovarian expression is driven by distinct follicle cell- and germ line-specific enhancers. *Mech. Dev.* **47**, 241–251 (1994).
51. Bischof, J., Maeda, R.K., Hediger, M., Karch, F. & Basler, K. An optimized transgenesis system for *Drosophila* using germ line-specific phiC31 integrases. *Proc. Natl. Acad. Sci. USA* **104**, 3312–3317 (2007).
52. Brand, A.H. & Perrimon, N. Targeted gene expression as a means of altering cell fates and generating dominant phenotypes. *Development* **118**, 401–415 (1993).
53. Cordier, F., Hartmann, B., Rogowski, M., Affolter, M. & Grzesiek, S. DNA recognition by the brinker repressor—an extreme case of coupling between binding and folding. *J. Mol. Biol.* **361**, 659–672 (2006).
54. Ohshiro, T. & Saigo, K. Transcriptional regulation of breathless FGF receptor gene by binding of TRACHELESS/dARNT heterodimers to three central midline elements in *Drosophila* developing trachea. *Development* **124**, 3975–3986 (1997).
55. Nikaido, M., Tada, M., Takeda, H., Kuroiwa, A. & Ueno, N. In vivo analysis using variants of zebrafish BMPRIA: range of action and involvement of BMP in ectoderm patterning. *Development* **126**, 181–190 (1999).